Chemical Engineering Journal 160 (2010) 249–258

Contents lists available at ScienceDirect

Chemical Engineering Journal

journal homepage: www.elsevier.com/locate/cej

Oxidation of benzene over bimetallic Cu–Ce incorporated rice husk silica catalysts

Farook Adam*, Radhika Thankappan

School of Chemical Sciences, Universiti Sains Malaysia, 11800 Penang, Malaysia

ARTICLE INFO

Article history:
Received 29 July 2009
Received in revised form 21 January 2010
Accepted 25 February 2010

Keywords:
Rice husk silica
Cu–Ce catalysts
Benzene oxidation
Phenol
H_2O_2

ABSTRACT

Oxidation of benzene to phenol with 30% H_2O_2 in liquid-phase was carried out over a series of Cu–Ce incorporated rice husk silica catalysts using acetonitrile as solvent at 343 K under atmospheric pressure. Cu and Ce incorporated rice husk silica catalysts were prepared by the sol–gel technique using cetyltrimethyl ammoniumbromide as the template. These catalysts were labeled as RHA–10Cu5Ce, RHA–10Cu20Ce, and RHA–10Cu50Ce. TG/DTG analysis of the catalysts confirmed complete removal of the template at 773 K and all catalysts were X-ray amorphous even after 50 wt% cerium incorporation. The rate for benzene oxidation increased linearly with cerium incorporation and depended directly on H_2O_2 decomposition. The high activity and phenol selectivity observed under mild reaction conditions (343 K, atmospheric pressure) could be correlated to the enhanced textural properties such as the BET surface area (403–279 $m^2\,g^{-1}$) and large pore volume (0.90–0.54 $m^3\,g^{-1}$) of the catalysts. Conversion during catalytic performance followed the order RHA–10Cu50Ce > RHA–10Cu20Ce > RHA–10Cu5Ce while phenol selectivity followed the order RHA–10Cu20Ce > RHA–10Cu5Ce > RHA–10Cu50Ce. A redox mechanism between Cu^{2+}/Cu^{+} and Ce^{4+}/Ce^{3+} active centers on the silica surface was responsible for the high catalytic activity of 84% with 96% phenol selectivity given by RHA–10Cu20Ce.

1. Introduction

Benzene is a hazardous volatile organic compound (VOC) of many industrial processes and catalytic oxidation is considered as most promising method for its effective removal [1]. In addition, phenol, one of the important chemical intermediates for the synthesis of various industrial products such as agrochemicals, petrochemicals and plastics has been mainly manufactured using the conventional "cumene-process" which has several disadvantages [2]. Eventhough, the selectivity for the phenol is high, this process consists of three steps and produces acetone as a byproduct, which results in many difficulties due to economical and environmental concerns [3]. The direct oxygenation of the energetically stable benzene to produce phenol has been one of the most difficult oxidation reactions. Therefore, a one-step production of phenol by direct insertion of oxygen into the C–H bond of benzene ring is an attractive and challenging idea.

New catalytic systems have been developed for the oxidation of benzene to phenol both in fixed-bed and liquid-phase using N_2O, H_2O_2 or O_2 as an oxidant [4–7]. Various copper catalysts such as Cu–ZSM-5 [8] Cu/Al_2O_3 [9], Cu/APO-11 [10] and Cu/HMCM-41 [11] have been reported to be efficient systems for phenol production from benzene. However, these catalysts are prone to copper leaching during oxidation, which can be controlled by adopting specific preparation procedure and incorporating with other metals [12]. Association of two or more active metals can perform well in a reaction system with the enhanced degree of interaction of the components over a support with new redox and acid properties [13]. Ceria (CeO_2), is well known for its oxygen storage/release capacity due to the oxygen vacancies and changes in the redox state of cerium ($4^+/3^+$). This property makes ceria a better catalyst for the reduction of SO_2, NO, NO_x emissions and in catalytic oxidation [14]. Co/Ce–SBA-15 catalysts have shown to be good in the complete oxidation of benzene due to a synergy effect between the cobalt and cerium ions [15]. Mesoporous $CuO–CeO_2$ was found to be very active for the complete catalytic oxidation of benzene owing to its richer lattice oxygen species [16]. Djinovic et al. reported that $CuO–CeO_2$ catalyst under proper temperature treatment, showed better water gas shift activity due to increased acidity/basicity which enhanced the adsorption of CO on the catalyst surface [17]. A mixture of CuO/CeO_2 was demonstrated as a promising catalyst for the complete oxidation of CO and phenol in comparison with CuO on other supports [18]. The enhanced activity of these class of catalysts generally related to the strong interactions between Cu species and surface oxygen vacancies of Ce with facile electron interplay of Cu^{2+}/Cu^{+} and Ce^{4+}/Ce^{3+} redox couples [19].

The rice milling process generates an abundant rice husk waste. This is commonly utilized for agricultural purposes, additives and as reinforcing material [20]. Due to energy crisis, consumption of this biomass for alternative energy source has also become more

* Corresponding author. Tel.: +60 4 6533567; fax: +60 4 6574854.
E-mail addresses: farook@usm.my, farook_dr@yahoo.com (F. Adam).

1385-8947/$ – see front matter © 2010 Elsevier B.V. All rights reserved.
doi:10.1016/j.cej.2010.02.055

important. Burning of rice husk produces ash which is mainly composed of silica. The silica from rice husk can be easily extracted by an acid pretreatment which results in more than 95 wt% of amorphous SiO_2 [21]. Rice husk silica has been successfully used as support for the preparation of various metal catalysts for industrially important reactions [22,23]. Recently chromium incorporated rice husk silica was reported to give complete conversion of cyclohexane with H_2O_2 as oxidant under very mild conditions [24]. Herein the selection of rice husk silica to incorporate Cu–Ce as catalysts for the oxidation of benzene is a promising challenge in the present scenario of environmental pollution abatement.

In the present work we report high surface area Cu–Ce incorporated rice husk silica catalysts prepared by a template assisted sol–gel precipitation method. The catalysts were used in a one-step oxidation of benzene using H_2O_2 as the oxidant in acetonitrile. A detailed characterization study has been undertaken in order to investigate the influence of enhanced physical properties when Cu and Ce were present together in the silica matrix so as to find a correlation with catalytic performance in the oxidation reaction. It is of great interest to study these catalytic systems which make use of an agricultural waste rice husk as the silica source in order to produce high demand phenol by a one-step oxidation of benzene.

2. Experimental

2.1. Catalysts preparation

The rice husk (RH) was obtained from a rice mill in Penang, Malaysia. It was washed and rinsed several times with distilled water in order to remove the dirt. The washed RH was dried at room temperature for 24 h. About 30.0 g of clean RH was stirred in 750 mL of 1.0 M HNO_3 at room temperature for 24 h to remove metallic impurities. The acid treated RH was washed with distilled water until the pH of the rinse was constant. The RH was dried and burned in a muffle furnace at 873 K for 6 h to complete combustion. The white rice husk ash (RHA) obtained was used for the preparation of the catalysts.

About 3.0 g of RHA was stirred to dissolve completely in 1.0 M NaOH (300 mL) to obtain sodium silicate solution. Cetyltrimethyl ammoniumbromide (CTAB, R&M Chemicals, 98%), used as the structure directing agent was dissolved in the solution (SiO_2: CTAB = 1: 0.05) and titrated with 3.0 M HNO_3 or 3.0 M HNO_3 containing dissolved metal salts in the required quantity (10 wt% Cu^{2+}, $Cu(NO_3)_2{\cdot}3H_2O$ (R&M Chemicals, 99%) and 5, 20 and 50 wt% Ce^{4+}, $Ce(NO_3)_3{\cdot}6H_2O$) (Fluka Chemika, 98%) with constant stirring until pH 3. The gel was aged for 24 h, filtered, washed several times with distilled water followed by acetone and dried in an oven at 373 K for 24 h. The samples were calcined at 773 K in a muffle furnace in the presence of air. The xerogel obtained was ground to powder and labeled as RHS (rice husk silica), RHA–*x*Cu*y*Ce where *x* = 10 wt% Cu^{2+} and *y* = 5, 20, or 50 wt% Ce^{4+} respectively.

2.2. Characterization

The prepared catalysts were characterized by powder X-ray diffraction (Siemens Diffractometer D5000, Kristalloflex operated at 40 kV and 10 mA with nickel filtered CuKα radiation (λ=1.54 Å), N_2-sorption porosimetry (NOVA 2200e surface area and pore size analyzer, FT-IR spectroscopy (PerkinElmer System 2000, KBr pellet method), DR UV–vis spectroscopy (PerkinElmer Lamda 35, KBr as reference) and thermo gravimetric analyses in O_2 atmosphere (TGA/SDTA 851^e Mettler Toledo). The morphology and elemental loading were observed by scanning electron microscopy (Leica Cambridge S360), energy dispersive X-ray analysis (Edax Falcon System), inductively-coupled plasma-mass spectrometry (ELAN 6100, PerkinElmer) and transmission electron microscopy (Philips CM12).

2.3. Oxidation of benzene

The oxidation reaction was carried out in a 50 mL double neck round bottom flask connected with a reflux condenser and kept in an oil bath, the temperature of which was controlled by a thermocouple. In a typical reaction, the catalyst powder (70 mg, pre-dried at 383 K), was suspended in a mixture of acetonitrile (10 mL, 116 mmol, Lab-Scan Asia Co. Ltd., 99.7%) and benzene (2 mL, 11.2 mmol, Fisher Chemicals, 99.98%) and kept in the oil-bath. After attaining the required reaction temperature (343 K), H_2O_2 (5 mL, 22.4 mmol, R&M Chemicals, 30%) was added drop wise to the system with stirring (700 rpm). About 0.5 mL of solution was withdrawn at regular intervals and analyzed by GC using *o*-cresol (Riedel-de Haen, 99%) as an internal standard. The influence of reaction parameters such as temperature, nature of solvent, catalyst amount, H_2O_2 concentration, time, leaching and reusability were studied over RHA–10Cu20Ce unless otherwise specified.

To test metal leaching, the catalyst was filtered off after 30 min of reaction and the filtrate quickly subjected at the set reaction conditions for further oxidation to proceed.

To monitor the efficiency of H_2O_2 as an oxidant, the concentration of H_2O_2 was determined by iodometry. The amount of H_2O_2 was quantitatively analyzed by titration with sodium thiosulphate (0.1N) using starch as indicator in the presence of potassium iodide (1% w/v), sulphuric acid and ammonium molybdate. The self-decomposition of H_2O_2 was also monitored in acetonitrile without involving benzene and the catalyst. During oxidation reaction, aliquots of solution was taken and the titration were quickly performed.

The analysis of the oxidation products was done on a Clarus 500 (PerkinElmer) gas chromatograph using capillary column (Elite 5, 30 m length and 0.32 mm inner diameter) equipped with an FID detector. The set temperature program was; initial oven temperature −323 K for 3 min; ramp of 283 K/min; final oven temperature −503 K; with N_2 as carrier gas. Products were confirmed on GC-MS using an Elite 5 column equipped with a mass selective detector and helium as the carrier gas.

3. Results and discussion

3.1. Catalyst characterization

The wide-angle powder X-ray diffraction pattern of the catalysts together with rice husk silica is shown in Fig. 1. The XRD pattern shows that RHA and metals incorporated silica catalysts has amorphous characteristics which was observable as a broad peak in the 2θ region of 20–30° [25]. In the diffraction pattern, the plane corresponding to copper or cerium oxide crystallites are not observed for all Cu–Ce containing catalysts indicating good dispersion of the loaded metals on the high surface area silica matrix. However, an observed shift of the broad pattern for RHA–10Cu50Ce, to 2θ region of 25–35° can be due to the poor crystallization of CeO_2 with the increase in Ce loading. Thus, crystallites and amorphous phase of CeO_2 are present in this sample [26]. These reflections overlap with reflections of silica lamellar phase thus the well separated peaks due to copper/cerium oxide are not observable in any of the samples.

The N_2-sorption isotherms of all the catalysts are shown in Fig. 2. The isotherm of RHS exhibits a pore network with an abundance of silanol groups [27]. All the catalysts exhibit type IV isotherm curves with well-defined characteristic condensation step at $P/P_o \sim 0.3$–0.6. It clearly indicates that these materials pos-

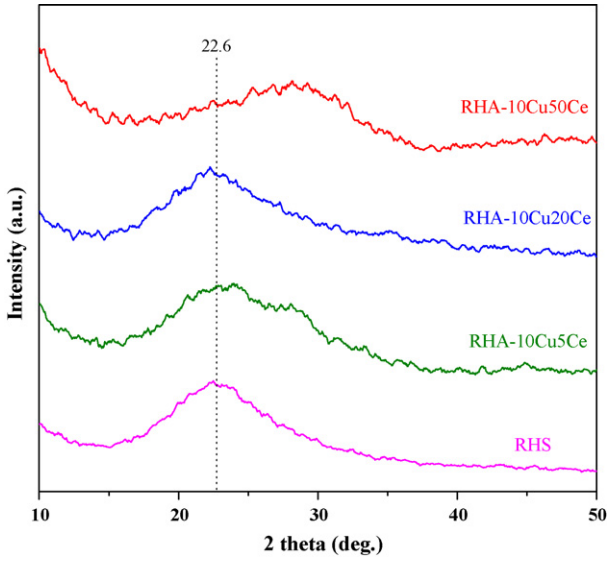

Fig. 1. The powder X-ray diffraction pattern for the prepared catalysts.

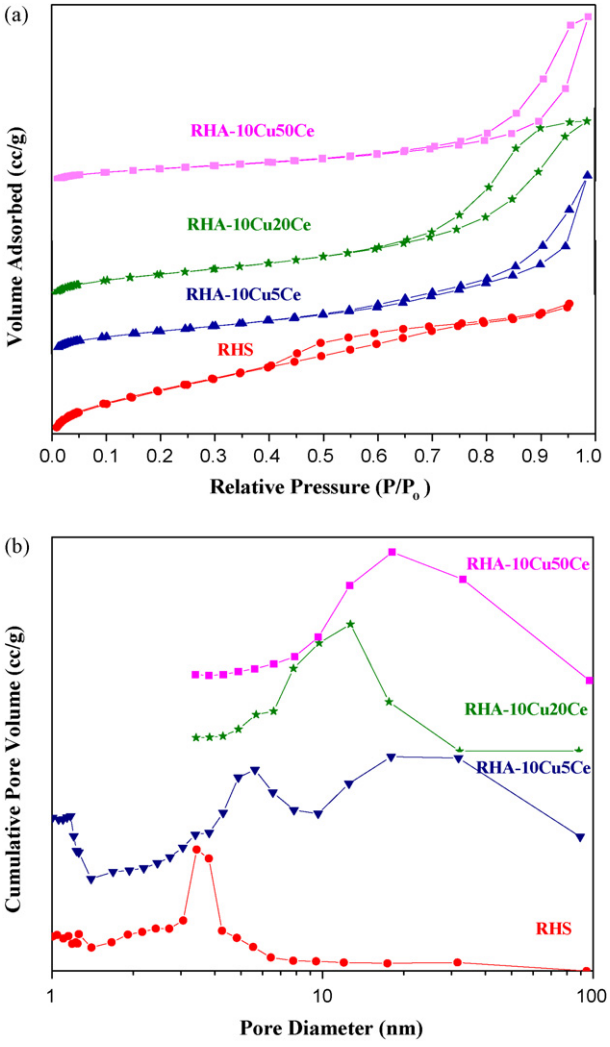

Fig. 2. The nitrogen sorption analysis (a) the adsorption-desorption isotherms of the catalysts and (b) the variation of pore diameter with respect to pore volume.

sess mesoporous structure [28]. The point of inflection increased progressively from $P/P_o = 0.4$ (RHS) to $P/P_o = 0.6$ (RHA–10Cu50Ce). This is characteristic of capillary condensation within the uniform mesopores of the materials. From the pore volume-size distributions for RHA–10Cu5Ce, appearance of various pores suggests the incorporation of Cu and Ce ions into silica framework to form highly dispersed species. A mixture of micropores and mesopores can be formed when cerium ion concentration is very low. Thus an irregularity suggests the co-existence of pores with different sizes probably by insertion of loaded metal ions [29]. In RHA–10Cu20Ce, pore-size distribution shows only mesopores with an average diameter of ~12.6 nm which decreases to ~9.6 nm upon increasing cerium content in RHA–10Cu50Ce. However, the pore size range is wider in RHA–10Cu50Ce. This can be due to the destruction of micropores and mesopores by insertion of more cerium ions into silica framework.

The textural properties such as specific surface area (S_{BET}), average pore diameters (d_{KJS}), specific pore volume (V_{pore}), relative pressure (P/P_o), and metal concentration analysis of the catalysts are summarized in Table 1. The results reveal that silica with a large BET specific surface area of 626 $m^2\ g^{-1}$ could be prepared from rice husk ash by a simple sol–gel precipitation method using CTAB as template. The surface area decreased upon Cu and Ce incorporation and reached 278 $m^2\ g^{-1}$ for RHA–10Cu50Ce as the Ce content increased to 50 wt%. The observed large specific surface area of all catalysts suggests the effectiveness of this method for the synthesis of mixed oxides with high specific surface area. The average pore volume (V_{pore}), increased up to RHA–10Cu20Ce and decreased with further increase of Ce to 50 wt%. Generally this behavior observed for mesoporous materials is explained by filling of micropores in the wall with the deposited metal ions [30]. Here a selective incorporation of cerium ions in competition with copper ions can be possible by the distinction of atomic radii of Ce^{3+}/Ce^{4+} (1.06–1.02 Å) and Si^{4+} (0.39 Å), which makes Ce–O bond length longer than that of Si–O bond [31]. Results representing the percent of metal loading in the bulk of the catalyst showed that cerium loading is higher while incorporated copper observed is very small, likely due to the difficulty for copper to diffuse inside the pores of the silica during the catalyst preparation procedure.

The FT-IR spectra of samples recorded in the 400–4000 cm^{-1} range are presented in Fig. 3(a) and (b). Fig. 3(a) shows the spectra of RHS and RHA–10Cu5Ce as synthesized along with the calcined catalyst. Fig. 3(b) depicts spectra recorded for various metal loaded catalysts after calcination. In all the spectra, a broad absorption band appeared for all catalysts around ~1640 and 3460 cm^{-1} corresponding to the vibrations of adsorbed H_2O molecule [32]. In RHA–10Cu5Ce–Synth., several absorption bands appeared at 2854 and 2925 cm^{-1} which were assigned to the stretching vibrations of C–H bonds in the methylene chains and at ~1479 cm^{-1} due to the deformation of $-CH_2-$ and $-CH_3$ groups of CTAB [33]. All the absorption bands corresponding to the template disappeared for RHA–10Cu5Ce-Calc which shows the complete removal of template molecule on calcination at 773 K. The strong bands at ca. 1095, 801 and 467 cm^{-1} agree with the typical Si–O–Si bond [34]. The band at ~974 cm^{-1} is due to the presence of Si–OH stretching vibrations [39]. The change in intensity with increasing cerium content indirectly proves the substitution of cerium ions in the silica framework. Replacement of Si with Ce results in a decrease in the intensity of the 974 cm^{-1} band showing the replacement of the Si–O–H groups with Si–O–Ce groups. Formation of Si–O–Ce bonds by replacement of Si–O–Si had been observed for Ce–MCM-41[35]. The increase in Si–O–Ce group supports the observed decrease of the average pore volume (V_{pore}) for RHA–10Cu50Ce.

Thermogravimetric analysis was performed from 293 to 1173 K under O_2 flow in order to determine the thermal treatment necessary to ensure complete removal of the organic template and/or

Table 1
The textural parameters and metal loading of catalysts.

Catalysts	S_{BET} (m^2/g)	V_{pore} (m^3/g)	d_{KJS} (nm)	Elemental (wt%)			
				Cu		Ce	
				EDX	ICP-MS	EDX	ICP-MS
RHS	625.8	0.60	3.4	–	–	–	–
RHA–10Cu5Ce	403.8	0.90	1.0	–	0.9	–	0.7
RHA–10Cu20Ce	328.8	0.95	12.6	1.9	1.6	17.1	13.8
RHA–10Cu50Ce	277.9	0.54	9.7	2.5	2.1	29.1	28.5
RHA–10Cu20Ce (after reaction)	–	–	–	0.0	0.5	11.6	9.8

any inorganic nitrates. Thermal analysis data of RHA–10Cu20Ce is shown in Fig. 4. The thermal pattern with a total weight loss of 15.9% revealed that nearly all the template and water formed due to condensation of silanol groups is lost at the calcination temperature of 773 K. The initial weight loss below 480 K (6.3%) is due to desorption of physisorbed water [36]. The weight losses in the range 480–720 K are mainly associated with the decomposition of the template, which further supports the observations evidenced from FT-IR spectra [37]. In the last step (723–773 K), the weight loss is mainly due to water loss formed by condensation of silanol groups. No significant weight loss was observed above 773 K. Based on these data, a temperature of 773 K was selected for the calcination of all the catalysts.

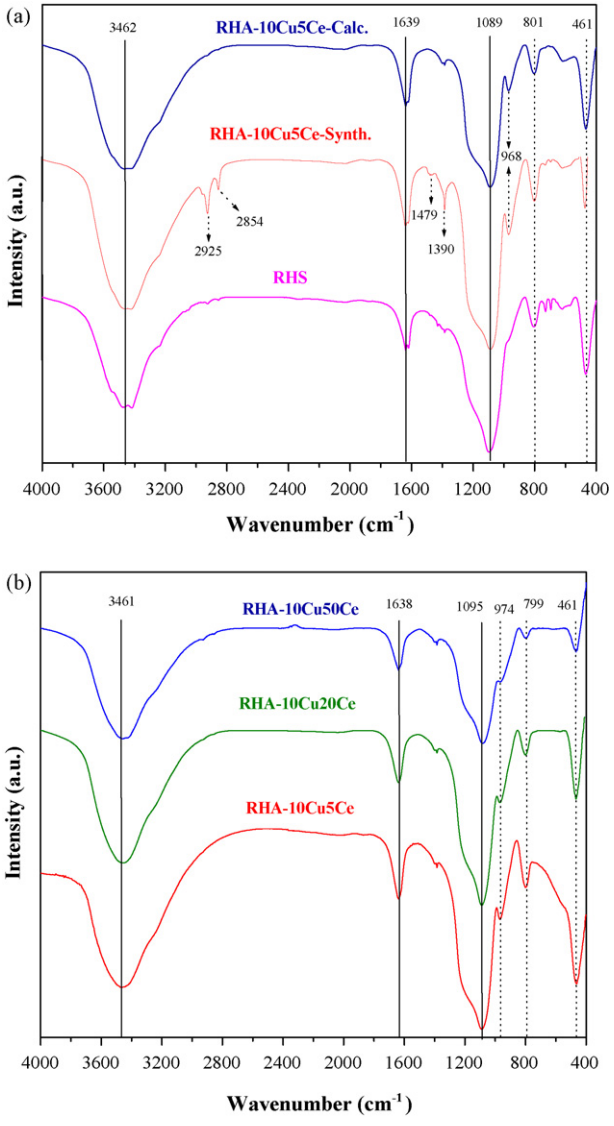

Fig. 3. The FT-IR spectra of (a) RHA–10Cu5Ce before and after calcination and (b) all the calcined catalysts in this study.

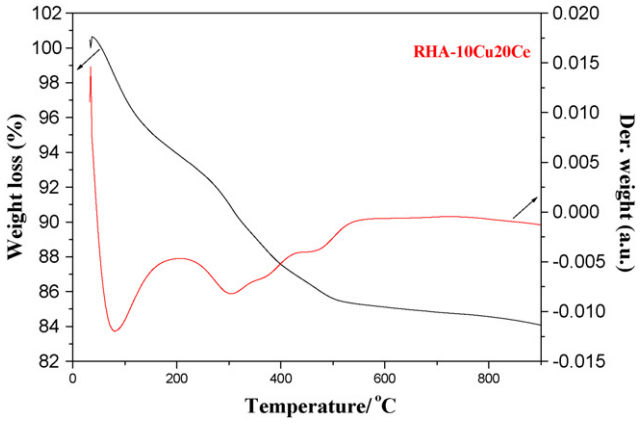

Fig. 4. The TG-DTG curve of RHA–10Cu20Ce.

DR UV–vis spectra of the catalysts were taken to establish structural environment and oxidation states of metals incorporated with silica are shown in Fig. 5. In the spectra, the absorption band at ~240 nm is due to the ligand to metal charge transfer between surface oxygen and isolated Cu^{2+} species [38]. The absorption band centered at ~300 nm arises from the metal charge-transfer transitions of O^{2-}–Ce^{4+} of well dispersed Ce^{4+} species in a tetra-coordinated environment [39]. With increasing cerium content (RHA–10Cu50Ce) both peak maxima merged together and the pattern became wider and shifted to longer wavelength. Even though XRD pattern suggested the presence of crystallites with increasing

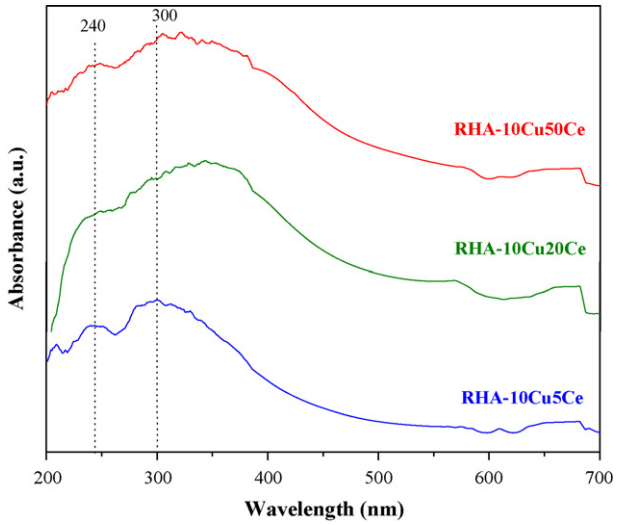

Fig. 5. The DR UV–vis spectra of the catalysts.

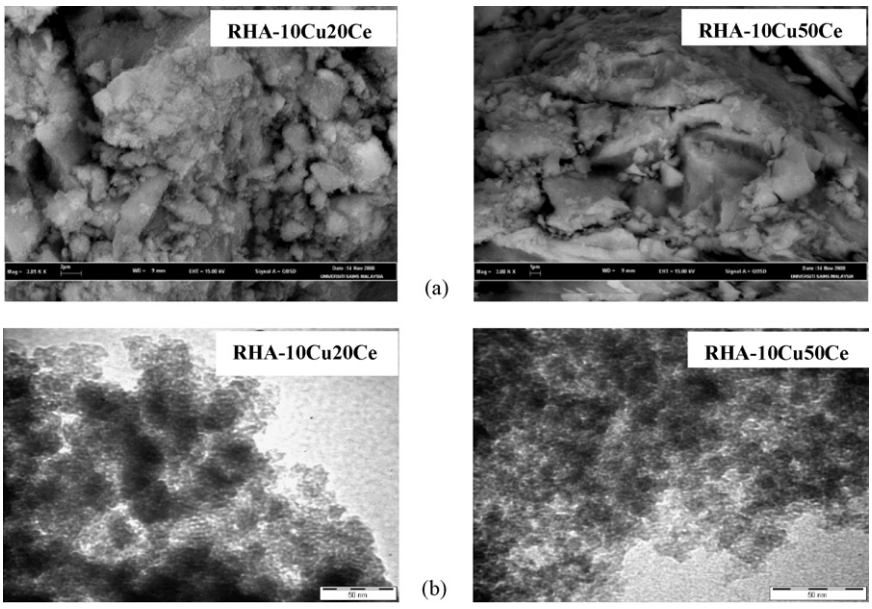

Fig. 6. The topographical and morphological pictures of RHA–10Cu20Ce and RHA–10Cu50Ce (a) SEM images and (b) TE micrographs.

Ce content (for RHA–10Cu50Ce), however, the absence of resolved characteristic bands of cerium crystallites in the range 350–700 nm ruled out the observation [31]. DR UV–vis data confirm the existence of highly dispersed Ce^{4+}–O^{2-} centre together with Cu^{2+} environment in the catalysts.

The topography and morphology pictured by SEM and TEM analyses for RHA–10Cu20Ce and RHA–10Cu50Ce are illustrated in Fig. 6(a) and (b) respectively. The SEM micrographs (Fig. 6(a)) show an agglomerated type for various metal loaded samples. The transmission electron micrographs shown in Fig. 6(b) reveal a partially ordered pore arrangements for Cu–Ce catalysts. This partially ordered characteristic nature can arise from the template micellar action during preparation of the catalysts. Materials that lack long-range order can be more active as heterogeneous catalysts in comparison to its ordered hexagonal analogues due to easy accessibility of the active centers to the substrate molecules [40].

3.2. Oxidation of benzene

The catalysts prepared were used in a one-step liquid-phase oxidation of benzene with H_2O_2 as the oxidant and acetonitrile as the solvent. The oxidation of benzene over Cu–Ce incorporated rice husk silica catalysts produced phenol as the major product along with only hydroquinone and 1,4-benzoquinone as byproducts. The equation for the catalytic oxidation is presented in Scheme 1.

The catalytic activity and phenol selectivity was found to be largely influenced by reaction parameters such as temperature, mass of catalyst, nature of solvent, concentration of H_2O_2 and time. The decomposition rate of H_2O_2 was determined by iodometric titration and it was found to play an important role in deciding the oxidant efficiency. Leaching of the metal ions from the catalytic system has also been investigated.

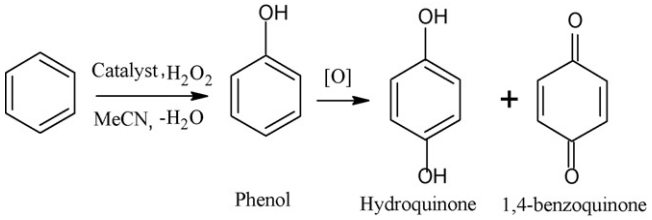

Scheme 1. The oxidation of benzene to phenol with the prepared catalysts.

3.2.1. The effect of varying reaction temperature

The effect of temperature on the oxidation of benzene was studied by varying the temperature from 303 to 353 K over RHA–10Cu20Ce (70 mg) with other parameters kept constant (H_2O_2 = 22 mmol; benzene = 11 mmol; acetonitrile = 116 mmol and reaction time of 5 h) and the results are shown in Fig. 7.

It can be seen that at room temperature (303 K) only 24.5% of benzene was oxidized, showing a very slow reaction. When the reaction temperature rose up to 343 K, a sharp increase in the oxidation activity (84.3%) and phenol selectivity (96.4%) was observed. Further increase of temperature to 353 K decreased the activity (81.2) as well as phenol yield (84.3%). This may arise due to the phenol being further oxidized to hydroquinone and 1,4-benzoquinone at the higher temperature. Vaporization of benzene can also occur at this temperature which can result in the decreased activity [41].

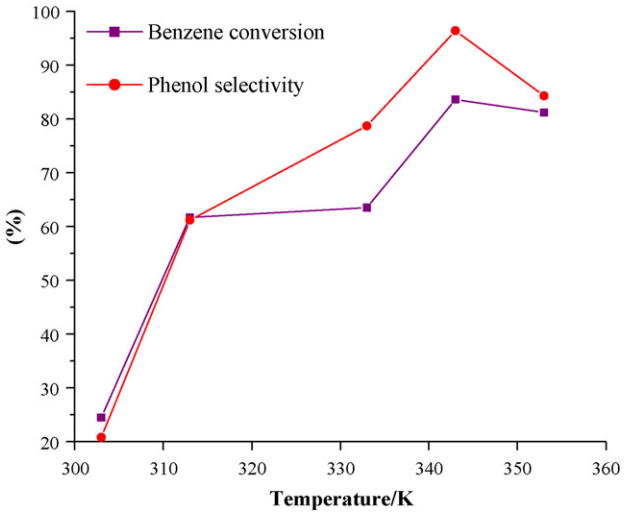

Fig. 7. The effect of temperature on benzene oxidation with RHA–10Cu20Ce as the catalyst (catalyst mass = 70 mg, benzene = 11 mmol, H_2O_2 = 22 mmol, acetonitrile = 116 mmol and reaction time = 5 h).

Table 2
The influence of solvent on benzene oxidation (mass of RHA–10Cu20Ce = 70 mg, benzene = 11 mmol, H_2O_2 = 22 mmol, solvent = 116 mmol, temperature of reaction = 343 K and time of reaction = 5 h).

Solvent	Conversion (%)	Selectivity (%)		
		Phenol	Hydroquinone	1,4-Benzoquinone
Acetonitrile	83.6	96.3	1.4	2.3
Water	77.1	11.6	–	88.4
Methanol	46.4	14.5	16.7	68.8
Acetic acid	78.7	35.3	12.6	52.1

It is also noticed that phenol, 1,4-benzoquinone and hydroquinone were detected as the only products with high selectivity towards phenol. No catechol or other oxidized products of phenol were observed with the catalysts studied. Zhang et al. suggested that Ce catalysts were most likely to form peroxide with low concentration of H_2O_2, which tends to form hydroquinone rather than catechol during oxidation of phenol [42]. Considering the results obtained, 343 K was the most suitable temperature for the catalysts in the present oxidation reaction studies.

3.2.2. The nature of solvent

The oxidation of benzene was carried out using various solvents such as acetonitrile, water, methanol and acetic acid on RHA–10Cu20Ce and the results are presented in Table 2.

Eventhough water as solvent gave high benzene conversion of 77.1%, the selectivity to phenol (11.6%) was much less due to further oxidation to yield mainly 1,4-benzoquinone (88.4%). Methanol showed less activity (46.4%) and phenol selectivity (14.5%) which was possibly due to the decomposition of solvent at the set reaction temperature since its boiling point is 337.7 K. Acetic acid showed high benzene conversion (78.7%) but the phenol yield (35.3%) was very low. The highest conversion of benzene (83.6%) and phenol selectivity (96.3%) was observed in acetonitrile. Acetonitrile, an aprotic solvent, can activate H_2O_2 by forming a perhydroxyl anion to produce a good oxygen transfer intermediate to initiate side-chain oxidation at the interface [43]. In addition, the oxidation activity in various solvents can relate to the effect of H_2O_2 consumption in its self-decomposition. Low self-decomposition rate may favour effective utilization of H_2O_2 as oxidant thus enhances the rate of oxidation reaction [41].

In this reaction with RHA–10Cu20Ce as the catalyst, it is interesting to note that depending on the product that is of interest, i.e. phenol or 1,4-benzoquinone, the reaction can be carried out using the appropriate solvent, i.e. water or acetonitrile—to obtain the desired product in very good yield. In the case of water as the solvent, hydroquinone was not detected. Resulting in a high yield of 1,4-benzoquinone (main product) and phenol as a side product which may be separated easily.

3.2.3. Concentration of H_2O_2

The concentration of H_2O_2 can have a marked influence on the oxidation of benzene. The effect of H_2O_2 concentration was studied by keeping the amount of benzene constant (11 mmol) over RHA–10Cu20Ce at 343 K in acetonitrile and the results are shown in Fig. 8.

No oxidation products were observed without the use of H_2O_2. An increase in H_2O_2 leads to a continuous growth of benzene oxidation, reaching a maximum value of 85.6% at benzene to H_2O_2 molar ratio of 1:4. The oxidation did not change much with increase in ratio from 1:2 to 1:4. However, a decrease in phenol selectivity occurred for 1:4 with maximum being 96.7% for molar ratio of 1:2. This decrease in phenol can be due to the increased formation of water in the reaction mixture, resulting in lowering of solubility, and/or to over-oxidation reactions of phenol to the byproducts

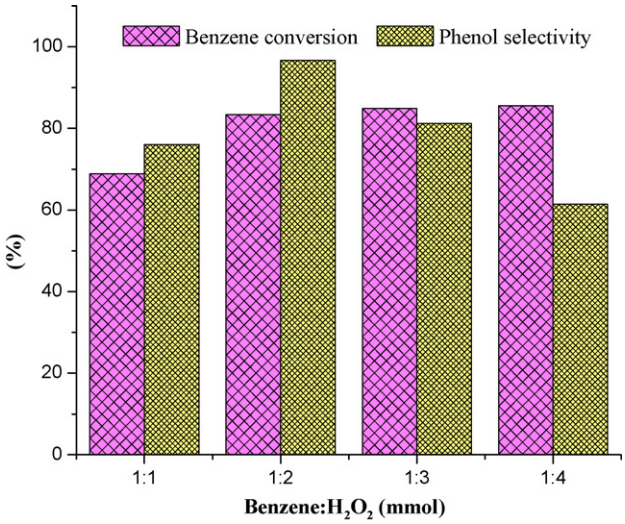

Fig. 8. The effect of H_2O_2 concentration on the conversion and selectivity of benzene: RHA–10Cu20Ce = 70 mg, benzene = 11 mmol, acetonitrile = 116 mmol, temperature = 343 K and time = 5 h.

at higher H_2O_2 concentrations [44]. Even though the theoretical molar ratio of benzene to H_2O_2 for the oxidation reaction is 1:1, here the result shows that H_2O_2 needed was double its stoichiometry. This can result from the fact that not all the H_2O_2 can take part in the oxidation due to its unavoidable self-decomposition under the reaction conditions [45].

3.2.4. Determination of decomposition of H_2O_2

An iodometric titration was used for the determination of H_2O_2 consumed as a function of temperature in order to compare its efficiency as an oxidant and the results are presented in Table 3.

Self-decomposition of H_2O_2 is unavoidable during an oxidation reaction. Thus an experiment was carried out at typical reaction conditions at room temperature with only H_2O_2 (22 mmol) in the presence of acetonitrile (10 mL) without involving benzene and catalyst to test the variation in the concentration of H_2O_2. Results showed a decrease in H_2O_2 concentration from 4.98 to 4.52 M, i.e. a reduction of 10% after 60 min. The decrease was due to self-decomposition. This supports the use of benzene to H_2O_2 molar ratio of 1:2. At room temperature (303 K), the catalytic activity increased linearly with decrease in the concentration of H_2O_2 and after 120 min about 62.6% of H_2O_2 remained. However, at the higher temperature of 343 K, consumption of H_2O_2 was found to be high initially and completely consumed at 120 min and conversion of benzene reached 78.9%. The results clearly indicate that the observed catalytic activity depends directly on the H_2O_2 consumption. Leng et al. concluded that during benzene hydroxylation over pyridine-heteropoly compounds, the yield of phenol was positively depended on the amount of H_2O_2 [46].

3.2.5. The effect of reaction time

Fig. 9 shows the conversion and the selectivity of benzene oxidation as a function of reaction time. As shown in figure, the amount of phenol formed increased with time initially, and reached 82.7% at 240 min of reaction. However, further oxidation of phenol to hydroquinone and 1,4-benzoquinone limits phenol selectivity to ~96.3% even after 300 min and did not increase with increase of time to 360 min. This can results from the oxidation of formed phenol as well as poisoning of surface sites by the reaction products which in turn block the active sites [47]. Based on the above results, the benzene conversion and phenol selectivity was found optimum for a reaction time of 300 min.

Table 3
The iodometric determination of H_2O_2 at different temperature and its effect on the conversion of benzene. RHA–10Cu20Ce = 70 mg, H_2O_2 = 22 mmol, benzene = 11 mmol and acetonitrile = 116 mmol.

Time (min)	Temperature			
	303 K		343 K	
	Concentration H_2O_2 [M]	Benzene conversion (%)	Concentration H_2O_2 [M]	Benzene conversion (%)
0	4.98	–	4.98	–
30	2.18 (4.66)[a]	5.2	1.43	45.6
60	2.04 (4.52)[a]	14.9	1.29 (4.84)[b]	69.9
120	1.86 (4.16)[a]	19.3	0.20 (4.78)[b]	78.9
300	1.12	24.5	0.00	83.6

[a] Self-decomposition analysis of H_2O_2 in acetonitrile.
[b] Iodometric titration of fresh 30% H_2O_2 without any reaction after keeping for prescribed time.

3.2.6. *The catalytic oxidation of substituted benzenes*

Substituted benzenes were subjected to oxidation under the optimized experimental conditions and the results are presented in Scheme 2.

Oxidation of various substituted benzenes resulted in selectively oxidised benzylic products along with trace amounts of ring hydroxylated products. Oxidation of toluene (conversion, 61.5%) and ethylbenzene (conversion, 65.2%) produced selectively, benzaldehyde (86.1%) and acetophenone (91.3%) respectively. Substitution of bulkier methyl and ethyl groups on the benzene ring reduced the possibility of ring hydroxylation. This is generally favoured in solution due to the formation of thermally stable benzylic intermediates [48].

To test the activity for alkane oxidation, the reaction was conducted using n-heptane under the same conditions. The product dictribution showed that the oxidation of n-heptane was moderate (conversion, 49.3%) with H_2O_2 and gave mainly substitution products such as ketones (71.2%), alcohols (16.5%), 3-hyddroxy heptane (7.8%) and heptanal (4.5%) over RHA–10Cu20Ce. No cyclization reaction was observed. It was interesting to note the formation of a mixture of chiral compunds, i.e. 3-hydroxy heptane, 4-methyl-2-hexanol and 6-methyl-3-heptanol. The formation of the last named product needs further verification. Trace amounts of aldoxime, $CH_3CH{=}NOH$ was also detected in the GC-MS. These products were formed by methyl migration of the intermediate redicals and involvement of the solvent, acetonitrile.

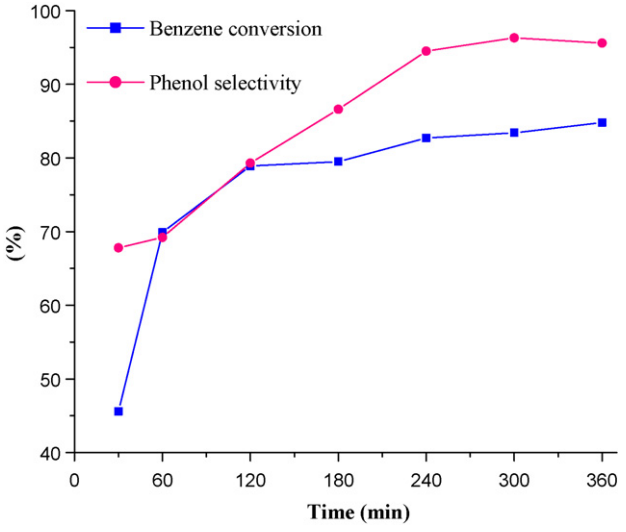

Fig. 9. The effect of reaction time on the percentage conversion of benzene. RHA–10Cu20Ce, 70 mg was used as the catalyst with benzene = 11 mmol, H_2O_2 = 22 mmol, acetonitrile = 116 mmol and temperature was maintained at 343 K.

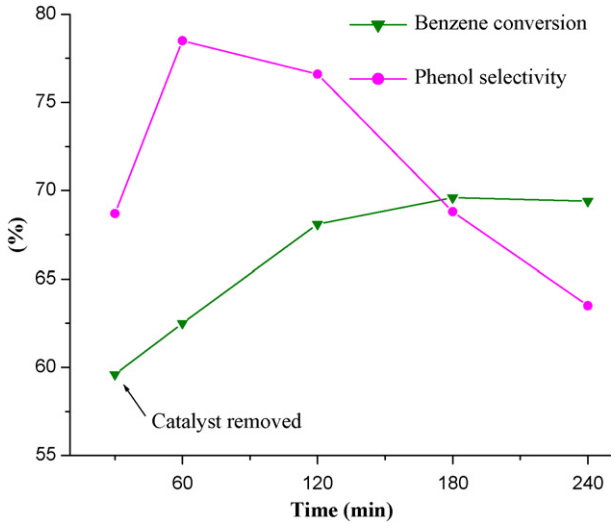

Fig. 10. Hot filtration results: RHA–10Cu20Ce = 70 mg, benzene = 11 mmol, H_2O_2 = 22 mmol, acetonitrile = 116 mmol and temperature = 343 K.

In comparison, the oxidation of heptane (conversion, 7.9%, 30 h) in high pressure reactor using silica gel supported vanadium oxo complex was reported to produce heptanols and heptanones mainly with negligible cracking and cyclization reactions [49].

3.2.7. *Leaching of metal and its effect on the catalytic performance*

Leaching of metal ions into the solution during oxidation reaction was studied by adopting hot filtration method [50]. At 30 min of reaction, the catalyst was removed by filtration while hot and the filtrate subjected to further reaction. The conversion and phenol selectivity was monitored for a time period of 240 min and is shown in Fig. 10.

At 30 min of typical reaction time, conversion was 59.6% with phenol selectivity of 68.7%. Resubmission of the hot filtrate under the same reaction conditions (without the catalyst) showed that the reaction continued slowly until the percentage conversion reached 68.1% and phenol yield attained 76.6%. No further increase in the conversion was observed. However, the phenol yield was observed to decrease to 63.5% over the next 240 min as a result of the formation of secondary oxidation products such as 1,4-benzoquinone and hydroquinone. Release of small amounts of loosely bound copper/ceria active centres on the surface of the catalyst during the oxidation could have resulted in the progressive increase in the conversion up to the first 120 min. However, the percentage conversion did not increase after 120 min, suggesting that not much leaching of active centres took place in accoradnce with usually observed phenomenon [51]. Chemical analyses of the filtered cata-

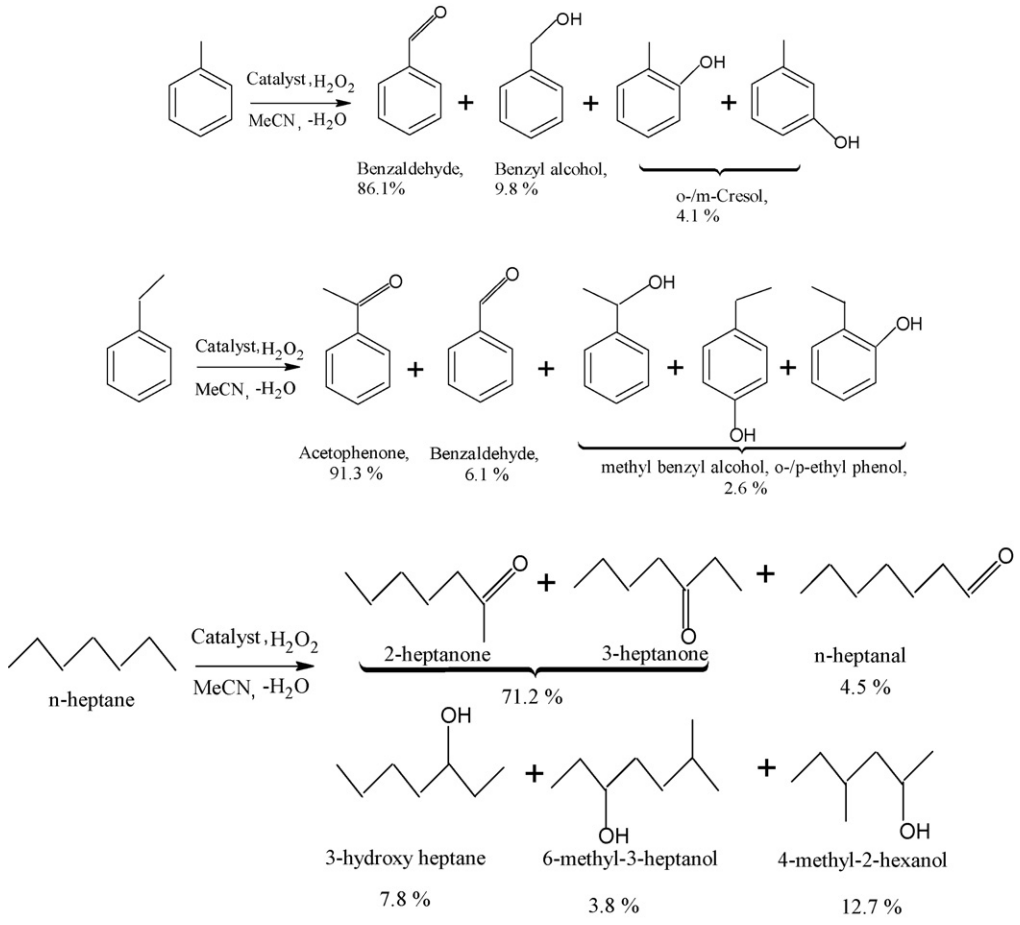

Scheme 2. The oxidation of toluene, ethylbenzene and n-heptane over RHA–10Cu20Ce (70 mg), substrate = 11 mmol, H_2O_2 = 22 mmol, acetonitrile = 116 mmol, temperature = 343 K and reaction time = 5 h.

lyst shows a decrease in the amount of Cu and Ce after the reaction (Table 1). Even though leaching of some metal was observed, the catalysts could be reused without much reduction in activity and phenol selectivity.

3.2.8. The catalytic oxidation under different metal loadings

Benzene was oxidized using catalyst with different metal loadings under the optimum reaction conditions found for RHA–10Cu20Ce. The results are shown in Table 4.

The oxidation of benzene over different metal loaded catalysts resulted in the same products. However, the selectivity for phenol was significantly lower and as a consequence a higher percentage of hydroquinone and 1,4-benzoquinone were obtained.

The catalytic systems containing only the mono-metal ceria (RHA–20Ce) or copper (RHA–10Cu) showed low activity and phenol selectivity in comparison to the bimetallic range of catalysts.

Table 4
The oxidation of benzene over catalyst with different metal loading.

Catalyst	Conversion (%)	Selectivity (%)		
		Phenol	Hydroquinone	1,4-Benzoquinone
RHA–10Cu5Ce	74.1	80.4	6.5	13.1
RHA–10Cu20Ce	83.5	96.4	1.4	2.3
RHA–10Cu50Ce	93.6	71.4	12.0	16.6
RHA–20Ce	23.5	34.6	25.8	39.6
RHA–10Cu	47.7	79.4	15.8	4.8
RHS	–	–	–	–

Catalyst = 70 mg, benzene = 11 mmol H_2O_2 = 22 mmol, acetonitrile = 116 mmol, temperature = 343 K and time = 5 h.

The mono-metal catalyst, RHA–20Ce showed only 23.5% conversion with 34.6% phenol selectivity. However, RHA–10Cu converted 47.7% benzene to give a selectivity of 79.4% for phenol. The silica only catalyst, RHS did not show any activity towards benzene oxidation under the same reaction conditions. This is indicating that the coexistence of copper and ceria in the catalytic system was necessary for improving the oxidation of benzene.

When the amount of ceria increased from 5 to 50 wt%, the benzene conversion increased from 74 to 94 (%) with H_2O_2 in acetonitrile at 343 K. Among all the catalysts tested highest yield of phenol (96.4%) was observed for RHA–10Cu20Ce. Even though the conversion observed for RHA–10Cu50Ce was high (93.6%), selective formation of phenol was reduced to 71.4%. The catalytic oxidation followed the order RHA–10Cu5Ce < RHA–10Cu20Ce < RHA–10Cu50Ce while the order of phenol selectivity was RHA–10Cu50Ce < RHA–10Cu5Ce < RHA–10Cu20Ce. Highest phenol production was observed for RHA–10Cu20Ce.

The comparison of the catalytic activities of the as-prepared high surface area catalysts exhibits excellent benzene oxidation with high phenol selectivity. The difference in activity between the catalysts can be related to the different structural environment of active centers as observed with various physio-chemical analyses. Generally better performance of all the catalysts can be ascribed to the high specific surface area which can present more active centers to substrate molecules thereby increasing the activity. Furthermore, the benzene conversion of RHA–10Cu50Ce was slightly higher than RHA–10Cu20Ce despite its lower surface area, which suggests that the BET surface area is not the only factor in deciding the catalytic oxidation of benzene but related also to other surface conditions.

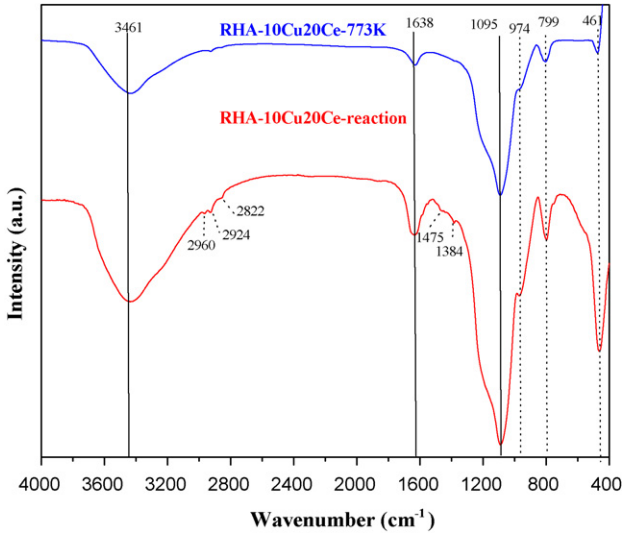

Fig. 11. The FT-IR spectra of RHA–10Cu20Ce after reaction and after calcination at 773 K.

As shown by DR UV–vis spectra the environment of Cu^{2+} and Ce^{4+} suggests the valency of Cu was +2 and Ce was +4 in the as-prepared RHA–*x*Cu*y*Ce catalysts. The XRD pattern showed no bulk CuO and CeO_2. Thus, a strong interaction of CuO and CeO_2 with SiO_2 is possible on the surface of the silica framework. In RHA–10Cu50Ce, formation of crystallite CeO_2 upon increasing the ceria loading may cause a reduction in the selective formation of phenol. The activity result of RHA–10Cu20Ce suggests that a specific concentration of Cu and Ce centers is necessary to produce phenol in high yield.

The presence of CuO together with the lattice oxygen rich CeO_2 can make the redox mechanism easier, and would lead to effective activation of the oxygen to oxidize the highly stable benzene molecule [52]. Todorova et al. reported that bimetallic Co–V–MCM-41 effectively catalyzed the oxidation of benzene to phenol (conversion 48.2%, phenol 81.2%) with H_2O_2 in acetonitrile at 343 K in 24 h [53]. Presence of highly dispersed V=O species on the surface of rice husk silica promoted ceria was found to produce phenol (100%) selectively from benzene oxidation (conversion, 21.4%) with H_2O_2 at 333 K in acetonitrile [54]. Recently a ternary metal oxide of $FeVCu/TiO_2$ was reported to give high phenol (70%) from benzene oxidation (conversion, 7.15%) with H_2O_2 in ascorbic acid. Incorporation of second and third metal improved the yield of phenol and also influenced the acid properties of the catalyst [55]. In the present reaction, a redox mechanism involving both Cu and Ce centers can operate with H_2O_2 to yield phenol as the major product with hydroquinone and 1,4-benzoquinone as the only byproducts.

3.2.9. Reusability and characterization of discharged catalyst

Reusability of the catalysts was tested by filtering the catalyst after first utilization. Filtered catalyst was washed with distilled water followed by acetone and activated at 773 K for 5 h before reuse. A decrease in conversion (77.1%, 5 h) was observed for second cycle with insignificant decrease in phenol selectivity (94.5%). However, for third cycle activity decreased to 65.7% with phenol selectivity of 92.1%. This can arise from loss of some active metal centers during various cycle of reaction as expected.

The FT-IR absorbance of the catalyst, RHA–10Cu20Ce after the first cycle of reaction with and without temperature treatment was recorded to monitor the presence of adsorbed benzene on the catalyst surface and the spectra are shown in Fig. 11.

The absorbance spectra of RHA–10Cu20Ce after reaction was recorded and it shows weak absorption bands in the range ~2950–2830 cm^{-1} which are due to the C–H stretching vibration of molecules adsorbed on the surface along with all typical bands of catalyst previously discussed in Fig. 3. In addition, a band appeared at ~1384 cm^{-1} indicating the presence of C–H bending vibration. Band at ~ 1475 is corresponding to the adsorbed aromatic rings. Upon calcination at 773 K, these bands disappeared. This suggests only weak adsorption of organic molecules took place on the catalyst surface during oxidation reaction [56]. High activity of studied catalysts thus can be correlated to this weak adsorption and can be reused after removal of adsorbed species by proper heat treatment of reacted catalysts.

3.3. Conclusions

A single step oxidation of benzene to phenol was carried out successfully over Cu–Ce incorporated rice husk silica as catalysts with H_2O_2. These catalysts show good catalytic performance (>70%) with high selectivity to phenol (~90%) due to a synergy effect between the Cu and Ce ions incorporated with silica. The observed high activity and selectivity of phenol could be correlated to the high surface area and pore volume and the good dispersion of loaded Cu and Ce ions on the amorphous silica. Oxidation on the surface of catalyst follow a redox mechanism involving Cu^{2+}/Cu^{+} and Ce^{4+}/Ce^{3+} sites.

Acknowledgement

We would like to thank the Malaysian Government for the Research University grants (Ac. No.: 1001/PKIMIA/814019 and 1001/PKIMIA/811092) which were used to support this work. R.T. thanks USM for providing a post-doctoral research fellowship.

References

[1] M.R. Morales, B.P. Barbero, L.E. Cadus, Combustion of volatile organic compounds on manganese iron or nickel mixed oxide catalysts, Appl. Catal. B: Environ. 74 (2007) 1–10.
[2] L.V. Pirutko, A.K. Uriarte, V.S. Chernyavsky, A.S. Kharitonov, G.I. Panov, Preparation and catalytic study of metal modified TS-1 in the oxidation of benzene to phenol by N_2O, Microporous Mesoporous Mater. 48 (2001) 345–353.
[3] G.I. Panov, A.S. Kharitonov, V.I. Sobolev, Oxidative hydroxylation using dinitrogen monoxide: a possible route for organic synthesis over zeolites, Appl. Catal. 98 (1992) 1–20.
[4] L.V. Pirutko, V.S. Chernyavsky, E.V. Starokon, A.A. Ivanov, A.S. Kharitonov, G.I. Panov, The role of α-sites in N_2O decomposition over FeZSM-5. Comparison with the oxidation of benzene to Phenol, Appl. Catal. B: Environ. 91 (2009) 174–179.
[5] H. Liu, Z. Fu, D. Yin, H. Liao, A novel micro-emulsion catalytic system for highly selective hydroxylation of benzene to phenol with hydrogen peroxide, Catal. Commun. 6 (2005) 638–643.
[6] M.H. Sayyar, R.J. Wakeman, Comparing two new routes for benzene hydroxylation, Chem. Eng. Res. Design 86 (2008) 517–526.
[7] Y. Ichihashi, T. Taniguchi, H. Amano, T. Atsumi, S. Nishiyama, S. Tsuruya, Liquid-phase oxidation of benzene to phenol by molecular oxygen over la catalysts supported on HZSM-5, Top. Catal. 47 (2008) 98–100.
[8] A. Kubacka, Z. Wang, B. Sulikowski, V.C. Corberan, Hydroxylation/oxidation of benzene over Cu–ZSM-5 systems: optimization of the one-step route to phenol, J. Catal. 250 (2007) 184–189.
[9] H. Kanzaki, T. Kitamura, R. Hamada, S. Nishiyama, S. Tsuruya, Activities for phenol formation using Cu catalysts supported on Al_2O_3 in the liquid-phase oxidation of benzene in aqueous solvent with high acetic acid concentration, J. Mol. Catal. A: Chem. 208 (2004) 203–211.
[10] X. Qi, J. Li, T. Ji, Y. Wang, L. Feng, Y. Zhu, X. Fan, C. Zhang, Catalytic benzene hydroxylation over copper-substituted aluminophosphate molecular sieves (CuAPO-11), Microporous Mesoporous Mater. 122 (2009) 36–41.
[11] J. Okamura, S. Nishiyama, S. Tsuruya, M. Masai, Formation of Cu-supported mesoporous silicates and aluminosilicates and liquid-phase oxidation of benzene catalyzed by the Cu-mesoporous silicates and aluminosilicates, J. Mol. Catal. 135 (1998) 133–142.
[12] T. Miyahara, H. Kanzaki, R. Hamada, S. Kuroiwa, S. Nishiyama, S. Tsuruya, Liquid-phase oxidation of benzene to phenol by $CuO–Al_2O_3$ catalysts prepared by co-precipitation method, J. Mol. Catal. A: Chem. 176 (2001) 141–150.
[13] E. Moretti, L. Storaro, A. Talon, P. Riello, R. Frattini, M. Lenarda, Effect of the synthetic parameters on the textural properties of one-pot mesoporous Al–Ce–Cu systems, Microporous Mesoporous Mater. 116 (2008) 575–580.

[14] C.C. Pantazis, D.E. Petrakis, P.J. Pomonis, Simultaneous and/or separate SO_2/NO reduction by CO over high surface area Cu/Ce containing mesoporous silica, Appl. Catal. B: Environ. 77 (2007) 66–72.
[15] Z. Mu, J.J. Li, H. Tian, Z.P. Hao, S.Z. Qiao, Synthesis of mesoporous Co/Ce-SBA-15 materials and their catalytic performance in the catalytic oxidation of benzene, Mater. Res. Bull. 43 (2008) 2599–2606.
[16] C. Hu, Q. Zhu, Z. Jiang, Y. Zhang, Y. Wang, Preparation and formation mechanism of mesoporous CuO–CeO_2 mixed oxides with excellent catalytic performance for removal of VOCs, Microporous Mesoporous Mater. 113 (2008) 427–434.
[17] P. Djinovic, J. Levec, A. Pintar, Effect of structural and acidity/basicity changes of CuO–CeO_2 catalysts on their activity for water–gas shift reaction, Catal. Today 138 (2008) 222–227.
[18] J. Zhu, Q. Gao, Zhi Chen, Preparation of mesoporous copper cerium bimetal oxides with high performance for catalytic oxidation of carbon monoxide, Appl. Catal. B Environ. 81 (2008) 236–243.
[19] A. Martınez-Arias, D. Gamarra, M. Fernandez-Garcı, A. Horne, P. Bera, Zs. Koppany, Z. Schay, Redox-catalytic correlations in oxidised copper-ceria CO-PROX catalysts, Catal. Today 143 (2009) 211–217.
[20] S. Chiarakorn, T. Areerob, N. Grisdanurak, Influence of functional silanes on hydrophobicity of MCM-41 synthesized from rice husk, Sci. Technol. Adv. Mater. 8 (2007) 110–115.
[21] F. Adam, K. Kandasamy, S. Balakrishnan, Iron incorporated heterogeneous catalyst from rice husk ash, J. Colloid Interf. Sci. 304 (2006) 137–143.
[22] F. Adam, I.A. Sugiarmawan, A porous ruthenium silica catalyst modified with amino benzoic acid for the oxidation of butanol with molecular oxygen, J. Porous. Mater. 16 (2009) 321–329.
[23] F. Adam, A.E. Ahmed, The benzylation of xylenes using heterogeneous catalysts from rice husk ash silica modified with gallium, indium and iron, Chem. Eng. J. 145 (2008) 328–334.
[24] F. Adam, P. Retnam, A. Iqbal, The complete conversion of cyclohexane into cyclohexanol and cyclohexanone by a simple silica-chromium heterogeneous catalyst, Appl. Catal. A 357 (2009) 93–99.
[25] T. Radhika, S. Sugunan, Influence of surface and acid properties of vanadia supported on ceria promoted with rice husk silica on cyclohexanol decomposition, Catal. Commun. 7 (2006) 528–533.
[26] S. Damyanova, C.A. Perez, M. Schmal, J.M.C. Bueno, Characterization of ceria-coated alumina carrier, Appl. Catal. A 234 (2002) 271–282.
[27] G. Marban, A.B. Fuertes, T. Valdés-Solís, Templated synthesis of high surface area inorganic oxides by silica aquagel-confined co-precipitation, Microporous Mesoporous Mater. 112 (1–3) (2008) 291–298.
[28] A.E. Ahmad, F. Adam, Indium incorporated silica from rice husk and its catalytic activity, Microporous Mesoporous Mater. 103 (2007) 284–295.
[29] N. Hosseinpour, A. Ali Khodadadi, Y. Mortazavi, A. Bazyari, Nano-ceria–zirconia promoter effects on enhanced coke combustion and oxidation of CO formed in regeneration of silica–alumina coked during cracking of triisopropylbenzene, Appl. Catal. A 353 (2009) 271–281.
[30] M. Kruk, M. Jaroniec, C.H. Ko, R. Ryoo, Characterization of the porous structure of SBA-15, Chem. Mater. 12 (7) (2000) 1961–1968.
[31] M.N. Timofeeva, S.H. Jhung, Y.K. Hwang, D.K. Kim, V.N. Panchenko, M.S. Melgunov, Y.A. Chesalov, J.S. Chang, Ce-silica mesoporous SBA-15-type materials for oxidative catalysis: Synthesis, characterization, and catalytic application, App. Catal. A 317 (2007) 1–10.
[32] L. Peng, W. Qisui, L. Xi, Z. Chaocan, Investigation of the states of water and OH groups on the surface of silica, Colloids Surf. A: Physicochem. Eng. Aspects 334 (2009) 112–115.
[33] W. Xue, H. He, J. Zhu, P. Yuan, FTIR investigation of CTAB–Al–montmorillonite complexes, Spectrochim. Acta Part A 67 (2007) 1030–1036.
[34] N. Venkatathri, Synthesis of mesoporous silica nanosphere using different templates, Solid State Commun. 143 (2007) 493–497.
[35] S.H. Park, B.Y. Song, T.G. Lee, Effects of surfactant/silica and silica/cerium ratios on the characteristics of mesoporous Ce–MCM-41, J. Ind. Eng. Chem. 14 (2008) 261–264.
[36] P. Renu, T. Radhika, S. Sugunan, Characterization and catalytic activity of vanadia supported on rice husk silica promoted samaria, Catal. Commun. 9 (2008) 584–589.
[37] D. Chandra, S.C. Laha, A. Bhaumik, Highly porous organic–inorganic hybrid silica and its titanium silicate analogs as efficient liquid-phase oxidation catalysts, Appl. Catal. A 342 (2008) 29–34.
[38] F.M.T. Mendes, M. Schmal, The cyclohexanol dehydrogenation on Rh-Cu/Al_2O_3 catalysts Part I. Characterization of the catalysts, Appl. Catal. A 151 (1997) 393–408.
[39] S.C. Laha, P. Mukherjee, S.R. Sainkar, R. Kumar, Cerium containing MCM-41-type mesoporous materials and their acidic and redox catalytic properties, J. Catal. 207 (2002) 213–223.
[40] J.C. Yu, A. Xu, L. Zhang, R. Song, L. Wu, Synthesis and characterization of porous magnesium hydroxide and oxide nanoplates, J. Phys. Chem. B 108 (2004) 64–70.
[41] K.M. Parida, D. Rath, Structural properties and catalytic oxidation of benzene to phenol over CuO-impregnated mesoporous silica, Appl. Catal. A 321 (2007) 101–108.
[42] Y. Zhang, F. Gao, H. Wan, C. Wu, Y. Kong, X. Wu, B. Zhao, L. Dong, Y. Chen, Synthesis, characterization of bimetallic Ce–Fe-SBA-15 and its catalytic performance in the phenol hydroxylation, Microporous Mesoporous Mater. 113 (2008) 393–401.
[43] T. Radhika, S. Sugunan, Vanadia supported on ceria: characterization and activity in liquid-phase oxidation of ethylbenzene, Catal. Commun. 8 (2007) 150–156.
[44] R.R. Fernandes, M.V. Kirillova, J.A.L. da Silva, J.J.R.F. da Silva, A.J.L. Pombeiro, Oxidations of cycloalkanes and benzene by hydrogen peroxide catalyzed by an $\{Fe^{III}N_2S_2\}$ centre, Appl. Catal. A 353 (2009) 107–112.
[45] M. Ishida, Y. Masumoto, R. Hamada, S. Nishiyama, S. Tsuruya, M. Masai, Liquid-phase oxygenation of benzene over supported vanadium catalysts, J. Chem. Soc., Perkin Trans. 2 (1999) 847–853.
[46] Y. Leng, H. Ge, C. Zhou, J. Wang, Direct hydroxylation of benzene with hydrogen peroxide over pyridine–heteropoly compounds, Chem. Eng. J. 145 (2007) 335–339.
[47] C. Liu, Z. Zhao, X. Yang, X. Ye, Y. Yu, Superconductor mixed oxides $La_{2-x}Sr_xCuO_{4\pm\lambda}$ for catalytic hydroxylation of phenol in the liquid–solid phase, Chem. Commun. (1996) 1019–1021.
[48] B. Chou, J.L. Tsai, S. Cheng, Cu-substituted molecular sieves as liquid phase oxidation catalysts, Microporous Mesoporous Mater. 48 (2001) 309–317.
[49] G.S. Mishra, A. Kumar, Silica gel supported [1,4-bis(salicylidene amino)-phenylene] vanadium oxo complex catalyst for the oxidation of *n*-heptane using molecular oxygen, J. Mol. Catal. A: Chem. 192 (2003) 275–280.
[50] R.K. Jha, S. Shylesh, S.S. Bhoware, A.P. Singh, Oxidation of ethyl benzene and diphenyl methane over ordered mesoporous M–MCM-41 (M = Ti, V, Cr): Synthesis, characterization and structure–activity correlations, Microporous Mesoporous Mater. 95 (2006) 154–163.
[51] A. Kong, H. Wang, X. Yang, Y. Hou, Y. Shan, A facile direct route to synthesize large-pore mesoporous silica incorporating high CuO loading with special catalytic property, Microporous Mesoporous Mater. 118 (2009) 348–353.
[52] G. Qi, R.T. Yang, Performance and kinetics study for low-temperature SCR of NO with NH_3 over MnO_x–CeO_2 catalyst, J. Catal. 217 (2003) 434–441.
[53] S. Todorova, V. Parvulescu, G. Kadinov, K. Tenchev, S. Somacescu, B.L. Su, Metal states in cobalt– and cobalt–vanadium-modified MCM-41 mesoporous silica catalysts and their activity in selective hydrocarbons oxidation, Microporous Mesoporous Mater. 113 (2008) 22–30.
[54] T. Radhika, S. Sugunan, Structural and catalytic investigation of vanadia supported on ceria promoted with high surface area rice husk silica, J. Mol. Catal. A: Chem. 250 (2006) 169–176.
[55] G. Tanarungsun, W. Kiatkittipong, P. Praserthdam, H. Yamada, T. Tagawa, S. Assabumrungrat, J. Ind. Eng. Chem 14 (2008) 596–601.
[56] V. Parvulescu, C. Anastasescu, B.L. Su, Bimetallic Ru–(Cr, Ni, or Cu) and La–(Co or Mn) incorporated MCM-41 molecular sieves as catalysts for oxidation of aromatic hydrocarbons, J. Mol. Catal. A: Chem. 211 (2004) 143–148.